

Waste water treatment by removal of heavy metals using EDTA-functionalized chitosan-graphene oxide nanocomposites

Asha Radhakrishnan^{1*}, Arya Sugathan², Deepa Vijayan², B. Beena³

Author Affiliations

^{1,2}Department of Chemistry, D.B. Pampa College, Parumala, Pathanamthitta, India

³Department of Chemistry, K.S.M.D.B. College Sasthamcotta, Kollam, India

Corresponding Author

*Asha Radhakrishnan, Department of Chemistry, D.B. Pampa College, Parumala, Pathanamthitta, India.

E-mail: ashagopan2009@gmail.com

Received on 13th January 2018

Accepted on 28th January 2018

Abstract

This study focuses on the preparation of Ethylenediaminetetraacetic acid (EDTA)-functionalized magnetic chitosan (CS) graphene oxide (GO) nanocomposites (EDTA-MCS/GO) by biogenic method and its removal efficiency for heavy metals namely, Pb(II) and As(III) from aqueous solutions. The synthesized nanocomposite was characterized by XRD, SEM, and FTIR analysis. The influence of various operating parameters, such as pH, metal ion concentration, and contact time on the removal of the metal ions, was investigated. The equilibrium data was evaluated by Langmuir, Freundlich and sips isotherms, while the heavy metal adsorption reaction kinetics was analyzed by Lagergren pseudo-first-order and pseudo-second-order kinetic models. The adsorption-desorption studies conducted over 6 cycles illustrate the viability and repeated use of the adsorbent for the removal of Pb(II) and As(III) from aqueous solutions.

Keywords: Adsorption, Heavy metals, Nanocomposites, Kinetics, Isotherms

1. INTRODUCTION

The discharge of wastewater containing heavy metals into the environment has increased continuously as a result of various human activities. Heavy metal contamination in such effluents presents a serious threat to the environment and human health because of their toxicity, non-biodegradability, carcinogenicity, and bioaccumulation in living organisms. Heavy metals such as Lead (Pb) and Arsenic (As) poses several risks to human health and long-term exposure in drinking water may cause cancer, muscular weakness, loss of appetite, and nausea. These issues require effective treatment of wastewater to decrease pollutants to acceptable levels. In this regard, many techniques have been developed for the removal of heavy metals from wastewater, such as chemical

precipitation, ion exchange, reverse osmosis, and adsorption. Among these, adsorption is the preferred technology because of its simplicity, effectiveness, and low cost [1].

In recent years, carbonaceous nanomaterials such as graphene oxide (GO), a two- or three dimensional nanosheet, have attracted the attention of researchers because of their unique properties and large composition diversity. The presence of a wide range of consecutive oxygen functional groups on the GO surface and large surface area provides abundant attachment sites for the functionalization of other compounds, such as chitosan (CS) and ethylene diamine tetra acetic acid (EDTA). This can ultimately increase the number of surface functional groups, which might enhance heavy metal adsorption. CS with primary amino groups is easily functionalized with different organic ligands, such as GO and EDTA, to improve its adsorption capacity. EDTA chelates with divalent metals, in which one carboxyl group is freely available and one water molecule is coordinated to the metal center [2].

In the present study EDTA–functionalized magnetic chitosan graphene oxide (EDTA-MCS/GO) nanocomposites is synthesized using biogenic method. Adsorption behavior of synthesized EDTA-MCS/GO nanocomposites for divalent Pb^{2+} and trivalent As^{3+} ions in aqueous solution is studied.

2. MATERIALS AND METHODS

2.1. Synthesis of EDTA-functionalized magnetic chitosan graphene oxide (EDTA-MCS/GO)

GO was synthesized from sugar cane bagasses oxidation. About 0.5 g of grounded sugar cane bagasse powder mixed with 0.1 g of ferrocene was taken in a china dish and directly kept in a muffle furnace at 300°C for 10 min under atmospheric condition. The black solid product was subjected for further analysis. The synthesis of EDTA-MCS/GO was a two-step process. In the first step, $FeCl_3$ (2 g) was dispersed in HCl. CS (2.0%) solution was obtained by dissolving low weight CS in HCl. GO solution, CS solution, and distilled water were added together and vigorously stirred for 1 h at room temperature. Then, NH_3 solution was added to induce the precipitation of a blackish material. The obtained product (MCS/GO) was washed several times with DI water and absolute ethanol, and finally dried in an oven. In the second step, EDTA and dried ground MCS/GO dispersions were mixed and allowed to react for 24 h at room temperature. Finally, the synthesized EDTAMCS/GO nanocomposite was oven dried at 600C then manually grinded into a fine powder for adsorption studies.

2.2. Adsorption Experiments: Batch type contact method

Adsorption experiments were carried out in a thermostatic water bath shaker at 150 rpm rate at a particular temperature for predetermined time intervals using 100ml clean and dried Stoppered bottles. The metal ion concentrations in liquid phase were determined by atomic absorption spectroscopic studies. The amount of metal ions adsorbed in (mg/g) at equilibrium (q_e) was calculated from the mass balance of initial and final metal concentrations in the aqueous phase. The amount of metal ion adsorbed at time q_e was calculated from mass balance equation.

$$q_e = \frac{(C_o - C_e)V}{m} \dots\dots\dots (1)$$

where q_e is the adsorbed metal ions per unit mass of adsorbent(mg/g) and V is the sample volume in L, m is the weight of the adsorbents.

The removal efficiency of various nanoadsorbents was calculated by using the equation,

$$\% \text{ removal} = \frac{(C_o - C_e)}{C_o} \times 100 \dots\dots\dots (2)$$

where, C_o and C_e are the initial and the equilibrium concentrations of heavy metal ions.

The quantity of metal ions adsorbed at selected time intervals was determined and used for kinetic analysis. Through the batch adsorption experiments it is possible to collect the details of the

applicability of adsorbent materials. But for studying the practical application in a bulk, continuous column studies are to be conducted in waste water effluents.

The adsorption conditions for the adsorbents were optimized by varying experimental parameters such as contact time, pH, initial concentration of adsorbate, pH, and adsorbent dose by batch method.

2.3. Instrumentation

The XRD measurement was performed on an XPERT-PRO powder diffractometer with Cu-K α radiation as the X-ray source in the 2θ range of $10-90^\circ$. The surface morphology was measured by a scanning electron microscope (SEM) of model JED-2300 system. FTIR spectra were recorded using Perkin-Elmer FTIR Spectrophotometer in the wave number range of 400 cm^{-1} to 4000 cm^{-1} by KBr disc method. Adsorption studies were carried out using GBC-AAS spectrometer having lamp current 5 milli ampere and a wave length 270nm.

3. RESULTS AND DISCUSSION

3.1. XRD Analysis

The XRD pattern of the GO is shown in Figure 1a. The peak at $2\theta = 11.6^\circ$ indicates that the agricultural sugarcane bagasse is fully oxidized into graphene oxide with the interlayer distance of 0.79 nm. This XRD pattern can be attributed to well graphitized two-dimensional structures made of GO sheets. The synthesized nanocomposite shows (Figure 1b), several sharp and strong diffraction peaks in, ranging from $2\theta = 30-70^\circ$, attributed to magnetic nature of nanocomposite. The XRD peak at $2\theta=30^\circ$ indicated the amorphous behaviour of CS. A peak around $2\theta=18^\circ$ might be the evidence of the presence of EDTA. These XRD peaks confirmed the formation of EDTA-MCS/GO nanocomposite [2].

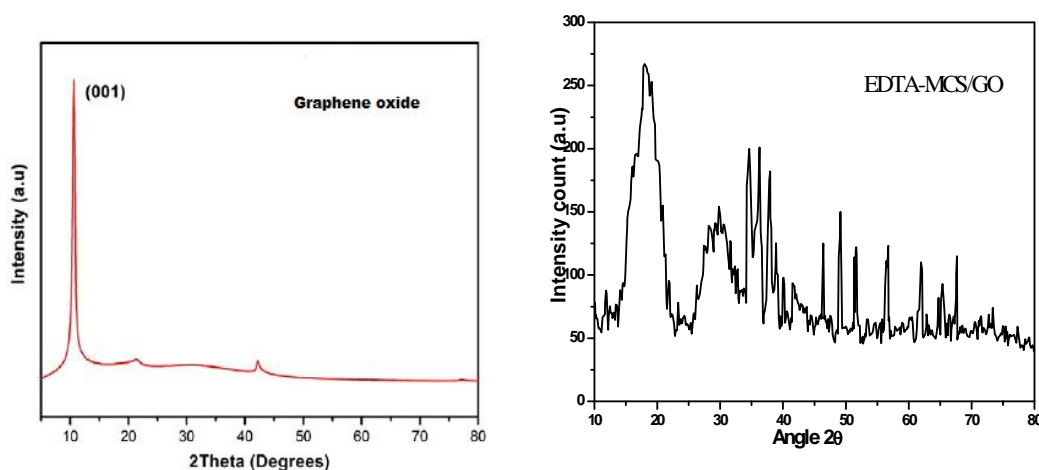


Fig.1: XRD spectrum of (a) Graphene Oxide (b) EDTA-MCS/GO nanocomposite

3.2. SEM Analysis

Surface morphologies and structures of the EDTA-MCS/GO nanocomposites were obtained from SEM analysis (Figure 2). The SEM image of GO (Figure 2a) revealed a sheet-like structure of sp^2 -hybridized carbon atoms with a smooth surface and crumpled edges. The SEM image of EDTA-CS (Figure 2b) revealed the spherical nanoparticles with smooth particle surface. The SEM image in Figure 2c shows small rounded magnetic chitosan (MCS) particles distributed roughly onto the GO surface. CS was well dispersed with GO and showed a close attachment, which indicated bonding between GO and CS. By adding EDTA, the size of magnetic particles increased. Therefore, in the surface of the GO sheets, comparatively large, rounded magnetic EDTA-CS particles were observed. This phenomenon increased the surface availability of the nanocomposites for adsorption and

prevented GO agglomeration. EDTA functional groups and amino groups present in CS could form chemical bonds with the GO sheet surface.

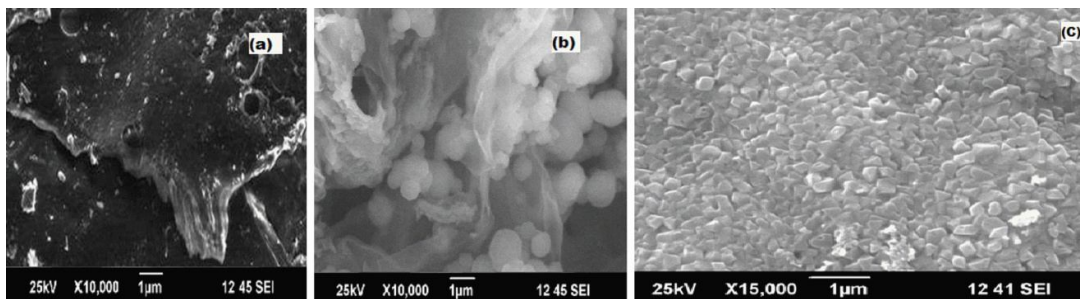


Fig. 2: SEM image of (a)GO,(b) EDTA-CS (c) EDTA-MCS/GO nanocomposites

3.3. FTIR Analysis

The FT-IR result shows (Figure 3) that EDTA-MCS/GO contains numerous oxygen and nitrogen functional groups. A broad band observed at 3386 cm^{-1} was assigned to O–H or N–H stretching vibrations from adsorbed H_2O or $-\text{NH}_2$ groups of CS on the surface of EDTA-MCS/GO. The band at 563 cm^{-1} was recognized as FeO bond stretching in EDTAMCS/ GO. The stretching vibration and bending vibration of the N–H bond appeared in a band at 1080 cm^{-1} , which was assigned to $-\text{NH}_2$ groups in EDTA or CS on the surface of EDTAMCS/GO. Another vibrational band at 1375 cm^{-1} was assigned to C–OH. A strong band at 1640 cm^{-1} was attributed to CO bond vibrations in carboxyl functional groups. Bands at 2920 and 2845 cm^{-1} resulted from C–H bonds in alkane groups. These O and N functional groups could act as available adsorption sites and play important roles in the removal of metal ions from aqueous solutions.

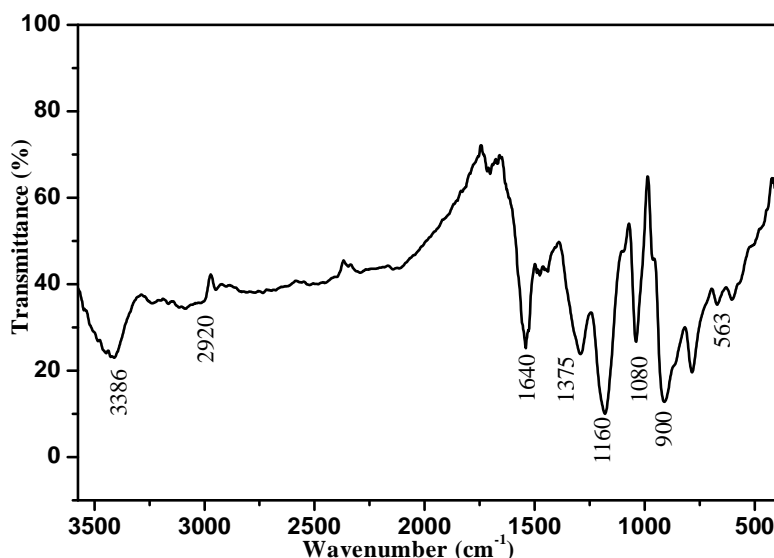


Fig. 3: FTIR spectrum of EDTAMCS/GO

3.4. Adsorption Studies

Present study focuses on the feasibility of synthesized EDTAMCS/GO as high efficient adsorbents for the removal of Lead ions (Pb(II)) and Arsenic ions (As(III)) from aqueous solutions. The effect of various operational conditions such as pH, adsorbent dosage and contact time was systematically studied. Adsorption kinetics and isotherm models were also analyzed to reveal the adsorption mechanisms.

The effect of pH on the adsorption capacity of metal ions such as Pb(II) and As(III) was evaluated in a pH range of 2.0 to 9.0 by agitating 100 ppm metal ion solution with 0.1g of EDTA-CS, GO and EDTA-MCS/GO separately. From Figure 4 it is observed that the percentage of adsorption of metal ions increased with increase in the solution pH for all adsorbents. The low adsorption in the acidic region can be attributed to the competition between hydrogen and metal ions for the same sites. The increase in pH makes the EDTA-MCS/GO surface more negative, thus enhancing electrostatic interactions between metal ions and the adsorbent, resulting in higher retention of metal species [3].

In the case of lead it exists as Pb^{2+} , $PbOH^+$ and $Pb(OH)^{3-}$ depending on pH. At lower pH value, low metal ion uptake was observed. At low pH values, the adsorbent is positively charged due to the presence of H^+ ions on its surface and hence offers repulsive force to approaching Pb^{2+} ions. However, more Pb^{2+} uptake is observed as the pH increases which are due to the fact that at high pH values, lead still has a net positive charge but exists as $PbOH^+$ while most active sites on the adsorbent are deprotonated. This leads to net attractive force that is responsible for high Pb removal from solution. But at elevated pH values i.e, in strong basic region, the uptake of metal ions decreased, may be due to the hydroxide formation. In the present study the removal efficiency in the case of all the three samples was found to increase with pH and attained maximum at pH 6 and then it was found to decrease. At all pH values EDTAMCS/GO showed maximum removal efficiency.

The pH of the solution was found to have a great effect on the adsorption of As(III) ions also. The adsorption increased sharply with pH and attained almost a constant value from pH 8 onwards and then showed a slight decrease in adsorption level [Figure 4]. The hydrolysis and precipitation of metal ions affect adsorption by changing the concentration and form of soluble metal species those are available for adsorption. Depending upon the pH of the solution, various species of arsenic can be formed during the hydrolysis. The hydrolysis extent of As(III) ions is unimportant up to approximately pH 8. [4]. In this case also at all pH values EDTAMCS/GO showed maximum removal efficiency. After each adsorption process, the final pH of the solution was recorded. It was found that after adsorption pH of the solution was lower compared to initial pH. This decrease in pH is an indication for ion exchange mechanism for removal of metal ions and the adsorption of metal ions onto EDTAMCS/GO surface by the release of H^+ ions [5].

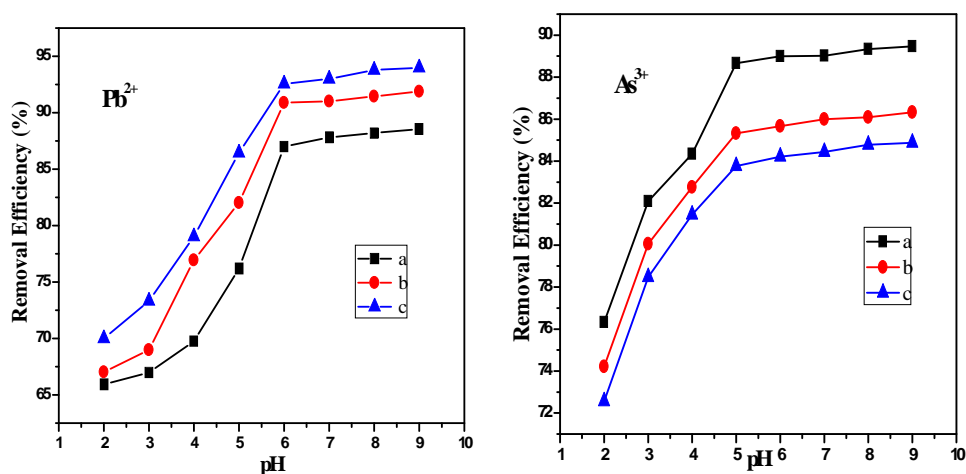


Fig. 4: Removal efficiency vs pH for Pb(II) and As(III)

The dependence of adsorbent dosage on metal ion adsorption was studied by varying the amount of adsorbents from 0.025 to 0.2 mgL⁻¹. From Figure 5, it can be observed that the removal efficiency of the adsorbents are enhanced by raising the adsorbent dosage and reached a saturation level at higher dosage. This is expected due to the fact that at higher concentrations of adsorbents greater is the availability of exchangeable sites for the ions. But increase in dosage beyond a certain level results

in no further increase in adsorption, may be due the fact that the amount of ions bound to the adsorbent and the amount of free ions in the solution remains constant [6].

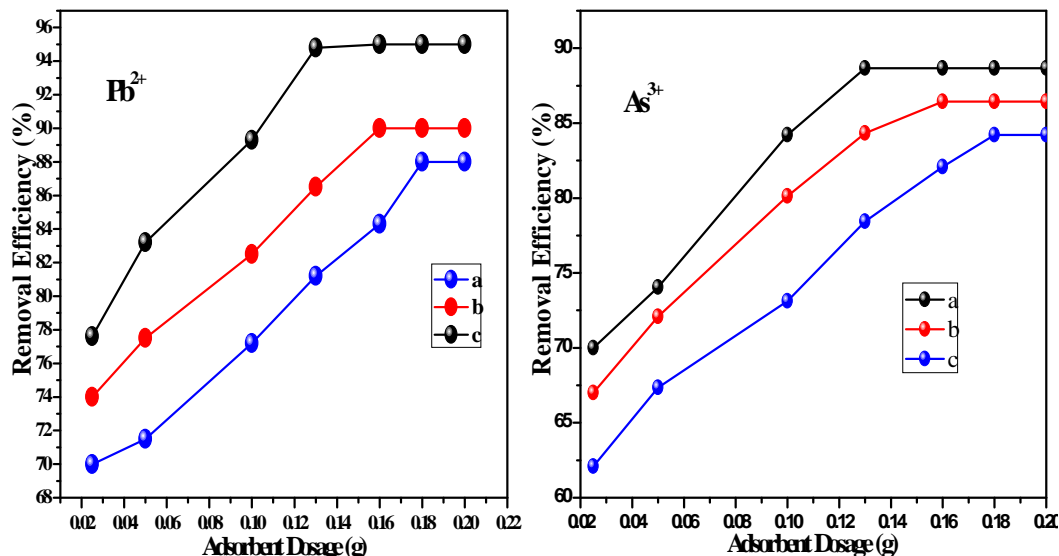


Fig. 5: Removal Efficiency vs adsorbent dosage for Pb(II) and As(III)

The dependence of adsorption capacity of EDTAMCS/GO on the initial concentrations of Pb(II) and As(III) ranging between 50 to 200 mg/L using 0.1 gm of the adsorbent is represented in Figure 6. The adsorption capacities increased steadily with increase in metal ion concentrations. The increase in the concentration gradient acts as a driving force for the adsorption process. When the concentration of metal ions increases, the active sites of EDTA-MCS/GO are surrounded by more metal ions, and the number of metal ions competing for available binding sites increases leading to an increased uptake of metal ions from the solution. Therefore the value of q_e increased with increase of initial metal ion concentration (C_0). It is also evident that adsorption capacity of EDTA-MCS/GO is higher as compared to EDTA-CS and GO; this is because of the presence of more active sites in EDTA-MCS/GO.

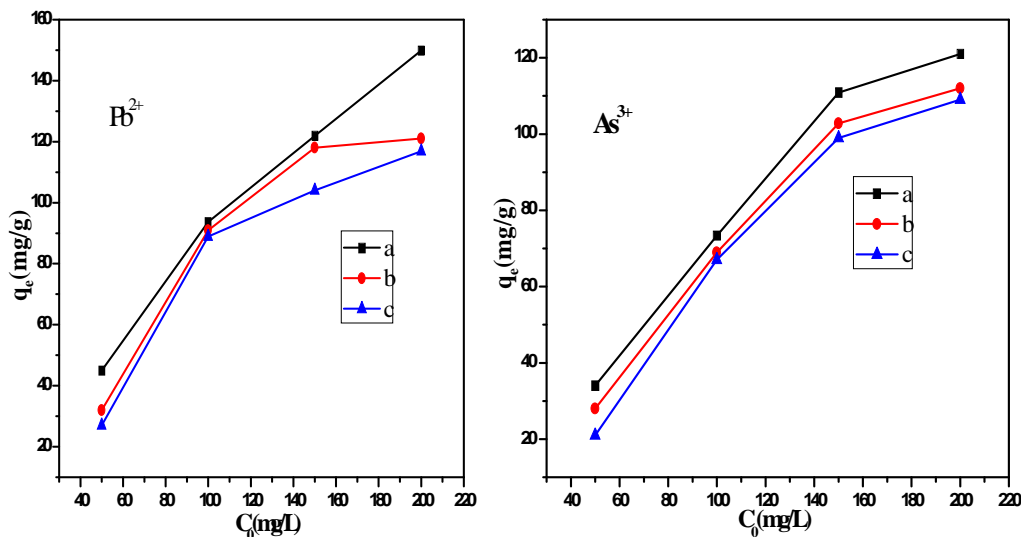


Fig. 6: Adsorption efficiency vs initial metal ion concentrations for Pb(II) and As(III)

The kinetic data were analyzed using the pseudo-first-order and pseudo-second- order kinetic models for EDTA-MCS/GO [Figure 7].

The kinetic data were analyzed using the following pseudo-first-order and pseudo-second-order kinetic models:

$$q_t = q_e(1 - e^{-k_1 t}) \quad \dots\dots\dots (3)$$

$$q_t = \frac{k_2 q_e^2 t}{1 + k_2 q_e t} \quad \dots\dots\dots (4)$$

where q_e and q_t are the amounts of solute adsorbed per unit mass of the adsorbent at equilibrium and time t (min), respectively, k_1 is the pseudo-first-order rate constant (min^{-1}) and k_2 is the pseudo-second-order rate constant of adsorption (g/mg/min). The pseudo-first-order and pseudo-second-order kinetic parameters were estimated from the experimental data using non-linear curve fitting procedure and the results are given in Table 3.3. The pseudo-first-order equation showed a poor correlation with experimental data, whereas the pseudo-second-order equation indicated a good correlation as indicated by a lower value of χ^2 and higher value of R^2 (nearing unity). In addition, q_e , which is the adsorption capacity, agreed very well with both the experimental and calculated values. The kinetic data indicates that the adsorption process is controlled by pseudo second-order equation. Also, this suggests the assumption behind the pseudo-second-order model that the metal ion uptake process is due to chemisorptions involving valence forces through the sharing or exchange of electrons between adsorbent and adsorbate [7].

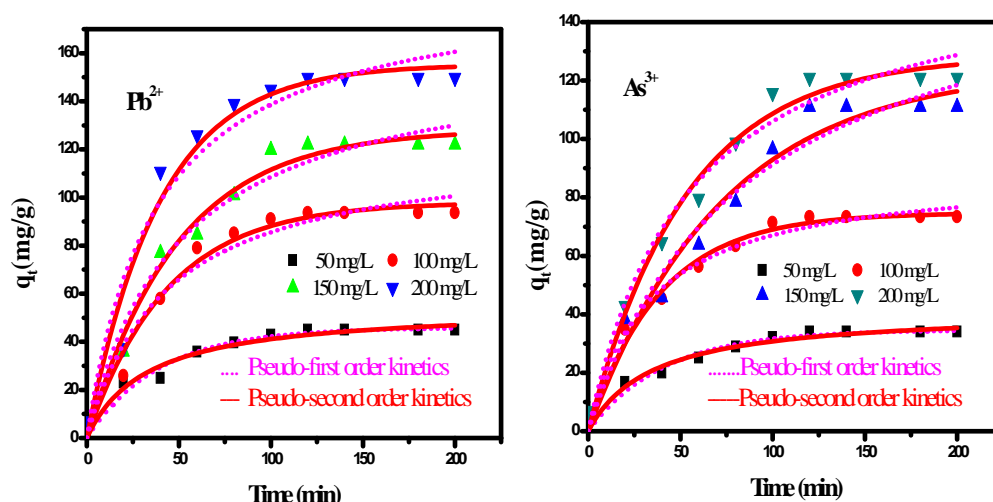


Figure 7: Kinetic plots for Pb(II) and As(III)

Table 1: Kinetic parameters for the adsorption of Pb(II) and As(III)

Metal ion	q_e (mg/g)	Pseudo-first-order				Pseudo-second-order			
		q_e (mg/g)	k_1 /min	R^2	χ^2	q_e (mg/g)	$k_2 \text{ min}^{-1}$	R^2	χ^2
Pb(II)	Exp	54.6	0.02	0.96	3.5	45.82	0.5×10^{-4}	0.96	0.61
	44.98	122	0.02	0.97	6	97.99	0.1×10^{-4}	0.95	0.23
	93.65	162.11	0.02	0.98	8	128.32	0.1×10^{-4}	0.96	0.57
	121.91	190.61	0.01	0.95	9	155.32	0.1×10^{-4}	0.99	0.17
As(III)	34	41.44	0.02	0.96	3.5	34.59	0.6×10^{-4}	0.96	3.21
	73.33	89.66	0.02	0.98	8	74.69	0.3×10^{-4}	0.98	3.62
	110.91	163.65	0.01	0.96	4.7	124.22	0.4×10^{-4}	0.95	5.71
	121	168.81	0.01	0.98	2.9	128.47	0.1×10^{-4}	0.97	4.62

The adsorption of metal ion on EDTA-MCS/GO was examined by well-known models to interpret equilibrium isotherm data. The experimental data of equilibrium adsorption were analyzed using the non-linear forms of Langmuir, Freundlich and Sips, isotherm equations:

$$q_t = \frac{q_m b C_e}{1 + b C_e} \dots\dots\dots (5)$$

$$q_e = K_F C_e^{1/n} \dots\dots\dots (6)$$

$$q_e = \frac{Q_s K_s C_e^{1/n_s}}{1 + K_s C_e^{1/n_s}} \dots\dots\dots (7)$$

where q_e and C_e are the equilibrium concentrations when an adsorbate gets adsorbed onto the adsorbent and q_m denotes the maximum adsorption capacity and b is the Langmuir constant. k_F (function of energy of adsorption and temperature) and $1/n$ (also called as the heterogeneity coefficient) are the Freundlich constants. If the $1/n$ value is less than 1, then it can be assumed that the adsorbent material is heterogeneous in nature. Q_s , is the Sips maximum adsorption capacity, k_s is the Sips equilibrium constant and $1/n_s$ is the Sips model exponent.

The experimental and model fits of Langmuir, Freundlich and Sips isotherms of Pb(II) and As(III) adsorption onto EDTA-MCS/GO are shown in Figure 8. The isotherm constants were calculated using non linear regression analysis and the results are listed in Table 2. Here also the values of R^2 and χ^2 showed that the adsorption of metal ions onto EDTA-MCS/GO was best fitted with Sips isotherm model over the concentration ranges studied. Sips isotherm model is a combination of Langmuir and Freundlich adsorption isotherm models. At higher concentration Sips favors Langmuir model while at lower concentration it favors Freundlich model. The R^2 values for all the three isotherms models were beyond 0.99 which indicate the suitability of models in explaining adsorption mechanism. Lower value of χ^2 and higher value of R^2 show a very good mathematical agreement with Sips isotherm model. Sips isotherm gives the idea of multilayer adsorption at lower concentration and monolayer at higher concentration of the metal ion.

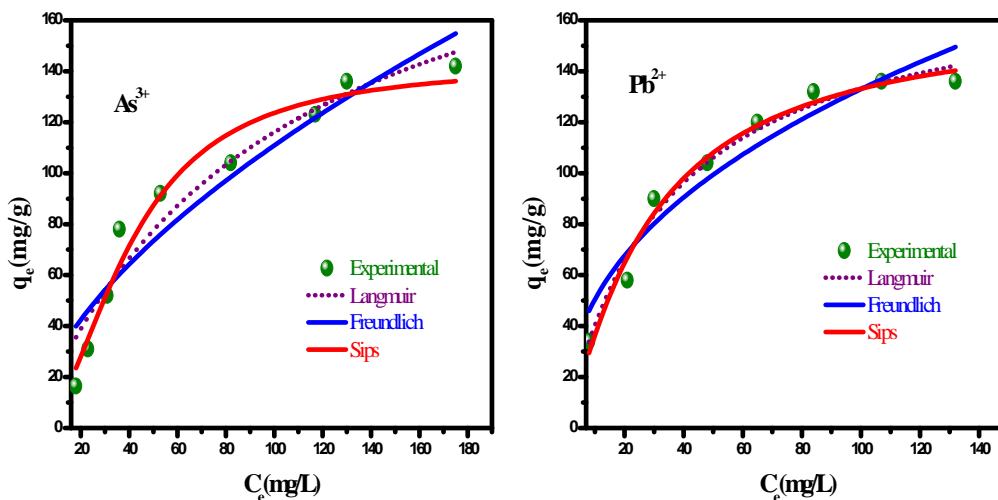


Fig. 8: Experimental and model fits of Langmuir, Freundlich and Sips isotherms of Pb(II) and As(III) adsorption onto EDTA-MCS/GO

Table 2: Langmuir, Freundlich and Sips isotherm constants for the adsorption of Pb(II) and As(III) onto EDTA-MCS/GO

		Pb(II)	As(III)
Langmuir	q_m mg/g	166.67	130.62
	b L/mg	0.19	0.01
	R^2	0.99	0.93
	χ^2	4.5	14
Freundlich	k_F mg $^{1-1/n}$ L $^{1/n}$ /g	44.47	7.12
	$1/n$	0.27	0.59
	R^2	0.98	0.88
	χ^2	2.0	2.2
Sips	Q_s mg/g	169.23	149.21
	K_s L/mg	0.10	0.005
	$1/n_s$	0.73	2.03
	R^2	0.99	0.95
	χ^2	1.1	8.3

In the present work the maximum adsorption capacity obtained using EDTA-MCS/GO for Pb²⁺ adsorption was 169.23 mg g⁻¹ and for As(III) it was 149.21 mg g⁻¹ under optimum conditions. This result suggests that the EDTA-MCS/GO prepared in the present study can be considered as a promising material for the removal of heavy metal ions from industrial waste water.

The desorption capacity of the prepared EDTA-MCS/GO was checked with HCl having different concentrations, ranging from 0.001 to 0.1 M . It was observed that the adsorbed Pb(II) and As(III) could be desorbed from the spent adsorbent using 0.1 M HCl and hence it could be used for the regeneration of EDTA-MCS/GO The adsorption–desorption process was carried out for six cycles with 0.1M HCl [Figure 9] and it was found that there was only a slight decrease in the adsorption capacity with respect to the regeneration cycles. However desorption capacity decreases to some extent because of the possible penetration of metal ions into inner cavities (pore diffusion or intraparticle diffusion). Therefore it could be included in the list of very effective adsorbent for Pb(II)and As(III) in real process such as industrial waste water treatment .

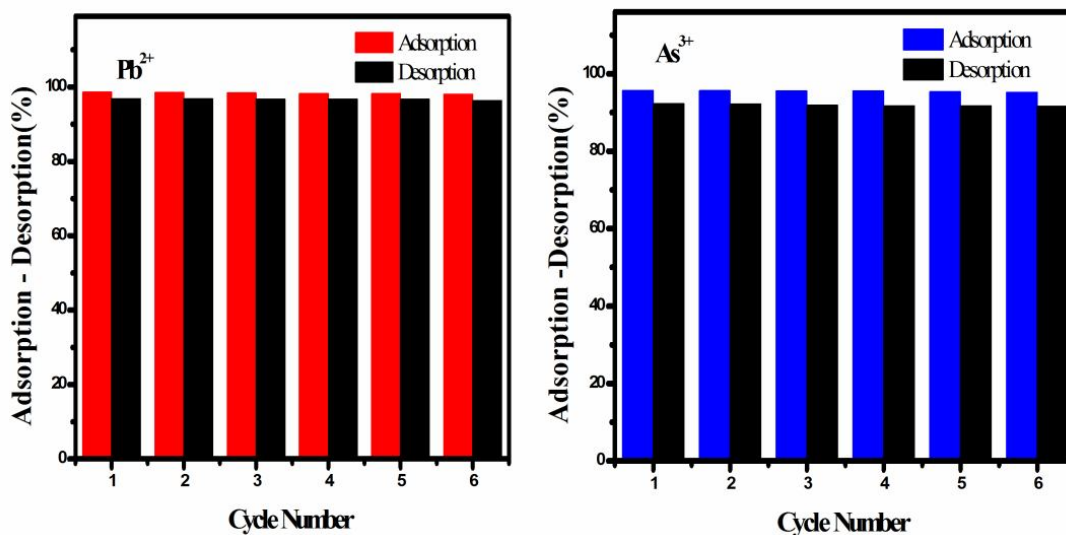


Fig. 9: Adsorption–desorption cycles for Pb(II) and As(III)

The practical efficiency and effectiveness of the adsorbents prepared were tested with industrial waste water. The collected waste water sample had Pb(II) and As(III) concentrations higher than the acceptable concentration for drinking water. Batch experiments conducted with industrial waste water showed that higher amount of adsorbent was needed compared to original metal ion solution. This discrepancy was due to the competitive adsorption of matrix ions with binding sites/screening effect by other metal ions.

4. CONCLUSION

This work demonstrated the efficient removal of divalent (Pb^{2+}) and trivalent (As^{3+}) metal ions using EDTA-MCS/GO nanocomposite. The synthesized nanomaterial was characterized by XRD, SEM, and FT-IR. The pseudo-second-order kinetic model gave better correlation with the adsorptions of all the metal ions than the pseudo-first order model. Sips isotherms were the best fits isotherm model for all metal ion adsorption. The synthesized nanocomposite exhibited a good regeneration capacity. Efficient removal of metal ions in real wastewater was also tested. Therefore, EDTAMCS/GO nanocomposite is a promising adsorbent metal ion removal from wastewater.

Acknowledgment

The authors wish to acknowledge Principal D.B. Pampa College for providing all facilities, SAIF Mumbai for SEM analysis and STIC Cochin for other instrumental analysis.

REFERENCES

- [1] Asha Radhakrishnan , Rejani P and Beena B., Main Group Metal Chemistry, 38, **2015**, 133-143.
- [2] Asif Shahzad, Waheed Miran, RSC Advances, 7, **2017**, 9764-9771.
- [3] Suleyman I and Yuksel A., Separation Science and Technology, 45, **2010**, 269–276.
- [4] Farooq U., Kozinski J.A., Khan M.A and Athar M., Bioresour. Technol., 101, **2010**, 5043–5053.
- [5] Rodriguez R.V., Cabrera M.E.M., Ponce H.E.E., Peraza E.F.H and Casarrubias M.L.B., Appl. Radiat. Isot., 70, **2012**, 872–881.
- [6] Yogesh K.K., Muralidhara H.B and Arthoba Y., Powder Technology, 239, **2013**, 208-216.
- [7] Asha Radhakrishnan., Rejani P., ShanavasKhan J and Beena B, Ecotoxicology and Environmental Safety, 133, **2016**, 457–465.